ORIGINAL ARTICLE

Lateral-torsional buckling of beams made of mono-symmetrical thin-walled sections

Maxime Vermeylen[1] | Marios-Zois Bezas[1] | Mathieu Crispin[2] | Jean-Pierre Jaspart[1] | Jean-François Demonceau[1]

Correspondence

Ir. Maxime Vermeylen
University of Liege
Steel and Composite Construction
Allée de la découverte 9 B52/3
Liege 4000, Belgium
Email: maxime.vermeylen@u-liege.be

[1] University of Liege, Liege, Belgium
[2] Stow International, Belgium

Abstract

Thin-walled cold-formed sections are extensively used as primary structural elements in storage system structures or steel houses, or as secondary elements like roof and wall systems, floor girders, etc. Despite their many advantages, such as transportability and lightweight, these members are usually susceptible to lateral-torsional buckling as they are not always laterally restrained.

This paper deals with the elastic stability of such beams and, in particular, is focusing on cross-sections that are symmetrical about their major axis only, like channel or sigma profiles, and loaded perpendicular to their axis of symmetry. Their stability has been studied analytically, in accordance to available provisions in the concerned codes, and numerically with two different finite element tools.

Keywords

Lateral-torsional buckling, LTB, Stability, Monosymmetric section, Thin-walled section

1 Introduction

Cold-formed thin-walled members have many advantages such as their reduced weight compared to the common hot-rolled profiles, the ease in transportation, the prefabrication process as well as the facility to reuse these elements. In addition, due to the great flexibility in shaping the sections, those can be of different geometrical characteristics, doubly symmetrical, monosymmetrical about one of their principal axes, or even unsymmetrical.

Due to the small thicknesses and high slenderness of the plates of these sections, local or even distortional buckling usually appears. Furthermore, as the majority of these elements exhibit open cross-sections with a low torsional inertia, the probability of lateral torsional buckling increases significantly.

Design rules and recommendations against lateral-torsional buckling (LTB) of thin-walled cold-formed beams can be found in both EN1991-1-3 [1] and EN1993-1-1 [2]. Furthermore, a formula to calculate the critical load of a monosymmetric member in bending can be found in the technical note CEN/TR 1993-1-103 [3]. However, its range of application is limited to the unique case where the section is loaded through its shear centre. Subsequently, its application field looks to be highly restricted and its use in other loading conditions is questionable.

Although a lot of studies have been performed by various researchers, they are mainly focusing on double symmetric or monosymmetric sections about their weak axis that are subjected to major axis bending. Numerous references can be found that are treating the problem of elastic member stability of I-shaped sections [4]-[5]-[6]. On the contrary, very few are referring to monosymmetrical sections about strong axis profiles subjected to strong axis bending. Seah et al. [7] investigates experimentally and analytically the buckling behaviour of channel beams subjected to bending only. Shan-shan et al. [8] propose an analytical study on lateral–torsional buckling of cold-formed channel section beams subjected to combined compression and bending about their major and minor axes. However, the complexity of the proposed differential equations makes them non suitable for practical design cases. Research performed by both Horacek ek al. [9] and Melcher et al. [10] concern the lateral-torsional buckling resistance of sigma sections with web holes, where the former investigates it numerically and the latter experimentally. Beyer et al. [11] study analytically and numerically the elastic instability of U members subjected to mono- and bi-axial bending due to end moments.

This paper, which involves numerical and analytical investigations, focuses on the lateral-torsional buckling of beams made of monosymmetrical sections around their strong axis in bending around this axis, particularly channel thin-walled cold-formed sections.

Within the present paper, the provisions available in the different codes are first briefly presented and discussed. As the forthcoming version of EN1993-1-3 and EN1993-1-1, namely prEN1993-1-3 [12] and prEN1993-1-1 [13] respectively, are available to the authors, their provisions are also checked and compared to the present ones. Then, numerical simulations were conducted by means of both FINELG [14] and Abaqus [15] software, and their results were compared and discussed with the analytical ones.

The current research takes place in an ongoing project funded by the Walloon Region (SPW - Belgium), involving industries, private research companies and the Steel and Composite Construction Department of the University of Liège.

2 Provisions available in the codes

In the following, the provisions against LTB found in the relevant normative documents are briefly presented and discussed. The specific design checks provided for purlins given in EN1993-1-3 are also commented.

2.1 LTB of member subjected to bending

As elements made of cold-formed thin-walled elements are studied, EN1993-1-3 is here considered. According to §6.2.4 of this code, the design resistance of a member in bending that is susceptible to LTB should be determined according to the design method provided in EN 1993-1-1, §6.3.2, using buckling curve b. The elastic critical moment should be based on gross cross-section properties, considering the loading conditions, the actual moment distribution, and the lateral restraints. As no ad-hoc formula is provided directly in EN1993-1-1, a reference to the technical report CEN/TR 1993-1-103 is made, where the case of beams with uniform cross-sections symmetrical about the major axis, as shown in Figure 1, is addressed.

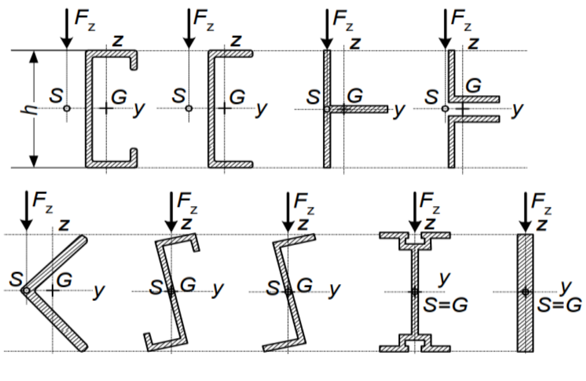

Figure 1 Beams with uniform cross-sections symmetrical about major axis, loaded in the plane going through the shear centre (figure extracted from [3])

More specifically, the critical moment M_{Cr} may be given by Equation (1).

$$M_{cr} = C_1 \cdot \frac{\pi^2 \cdot E \cdot I_z}{(k_z \cdot L)^2} \cdot \left[\sqrt{\left(\frac{k_z}{k_w}\right)^2 \frac{I_W}{I_z} + \frac{(k_z \cdot L)^2 \cdot G \cdot I_t}{\pi^2 \cdot E \cdot I_z} + \left(C_2 \cdot z_g\right)^2} - C_2 \cdot z_g \right] \quad (1)$$

where:

- C_1, C_2 are coefficients depending on the loading and support conditions that can be found for some usual loading cases in [3] or in few relevant National Annexes;
- k_z, k_w are effective length factors that depend on the support conditions at the extremities of the member and vary between 0.5 (fixed support) and 1.0 (free support);
- $z_g = (z_a - z_s)$ where z_a and z_s are the z-coordinates of the load application point and of the shear centre, respectively. These coordinates are positive if the load application point is in the compressed part and negative if it is in the tension part.

However, it is stated that the application of Equation (1) is limited: "*beams with uniform cross-sections, symmetrical about the major axis loaded perpendicular to their major axis in the plane going through the shear centre*". For the here considered cross-section shapes (i.e., C, Σ, etc.), this situation is rather theoretical as their shear centre is always located out of the cross-sectional area. As a result, most of the practical cases are not covered.

In Section 3, the field of application of Equation (1) and its use conditions will be further examined through several analytical and numerical investigations.

2.2 Design rules for purlins Z, C and Σ members restrained by sheeting

A specific design method to design Z, C and Σ purlins restrained by sheeting is proposed in §11.1 of prEN1993-1-3, where equations to check the stability of the free flange in compression are given. However, as these formulae account for the beneficial restraining effect of the sheeting, they are not suitable for simply supported members, and so they are not considered in this paper.

It must be noted that, regarding the LTB design provisions reported in this section, the authors have not revealed any significant difference between the current version of the norms and the forthcoming ones, apart from the equations notations which sometimes differ from one version to another.

3 Analytical and numerical investigations

Analytical calculations were firstly achieved for two simple successive study cases. Then, numerical studies were performed, and the results were compared to the analytical ones. These studies are presented in the following paragraphs. Both analyses are aiming to validate and further specifying the field of application of Equation (1).

3.1 Case study 1

3.1.1 Analytical calculations

A C-section member with a total length of 4000 mm and an elastic steel material law has been considered (E = 210,000 MPa). Table 1 summarizes the geometrical nominal gross section properties of the C-profile obtained with Calpro, a specific tool available in the FINELG software. The dimensions of the profile have been selected in such a way that no local and distortional buckling occurs according to the provisions of EN1993-1-3 (reduction factors are equal to 1.0) so as to minimize the parameters influencing the response of the beam.

Table 1 Gross cross-section properties of the studied section

Property		Value
Area	A	314.0 mm^2
Moment of inertia	I_y	165,787.0 mm^4
Moment of inertia	I_z	59,951.0 mm^4
Section modulus	W_y	5,526.0 mm^3
Torsion constant	I_t	418.0 mm^4
Warping constant	I_w	86,149,594.0 mm^6

The member is simply supported only at its extremities through fork supports and is subjected to two vertical loads at L/4 and 3L/4 as schematized in Figure 2; the corresponding bending moment diagram is illustrated too. In order to investigate the influence of the position of the vertical loads applied to the member on the critical LTB resistance, the six following application points, illustrated in Figure 3, have been considered:

1. At the shear centre (S);
2. At the centre of gravity (G);
3. At the top flange – left edge (TLE);
4. At the top flange – right edge (TRE);
5. At the bottom flange – left edge (BLE);
6. At the bottom flange – right edge (BRE).

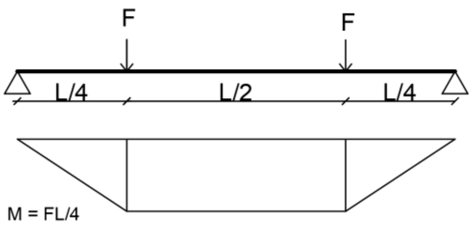

Figure 2 Static system and distribution of the bending moments along the studied member

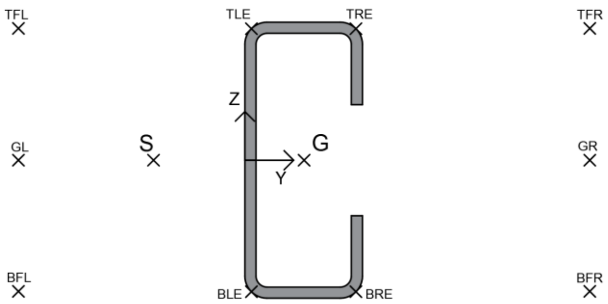

Figure 3 Considered application points of the vertical loads in the plane of the section

An analytical evaluation of the elastic critical moment of the member through Equation (1) is presented in Table 2 for the six different loading positions; even if, according to the technical report CEN/TR 1993-1-103, the application of Equation (1) is limited to situations where the loads are applied in the vertical plane passing through the shear centre (S). As the beam is assumed to be simply supported, k_z and k_w were taken equal to 1.0. As expected, the value of the critical bending moment varies according to the vertical position of the applied load (through the variation of z_g). The most unfavourable situation, corresponding to the minimum critical elastic bending moment, occurs when the force is applied at the top of the section, while the most favourable situation, i.e., when the critical elastic bending moment is maximum, corresponds to the cases where the force acts on the bottom flange of the section. It is obvious that the second case should be targeted by the designers. However, this is not always feasible due to the structural configurations.

Table 2 Analytical evaluation of the elastic critical moment for the 1st study case through Equation 1, where C1 and C2 are according to [16]

N°	Position of the loading	z_g	C_1	C_2	k_z	k_w	$M_{cr,an}$ [kNm]
1	S	0	1.04	0.42	1	1	0.61
2	G	0	1.04	0.42	1	1	0.61
3	TLE	$h/2$	1.04	0.42	1	1	0.52
4	TRE	$h/2$	1.04	0.42	1	1	0.52
5	BLE	$-h/2$	1.04	0.42	1	1	0.72
6	BRE	$-h/2$	1.04	0.42	1	1	0.72

3.1.2 Numerical simulations

In order to validate the analytical approach, linear buckling analyses with FINELG finite element software have been conducted. As local or distortional buckling is not deemed to occur due to the selected cross-section, 40 beam elements along the member's length have been used for these analyses. Three different situations have been considered in terms of coincidence or no coincidence of two reference lines: a line joining the punctual supports (named SL) and a line along which the loads are applied (named LL), as illustrated in Figure 4:

a. The SL and the LL coincide (and pass either through point G, S, TLE, BLE, etc) ;
b. The SL passes through the gravity centre G while the loads are introduced along a LL passing in one of the six here-above mentioned points;
c. The SL passes through the shear centre S while the loads are introduced along a LL passing in one of the same six points.

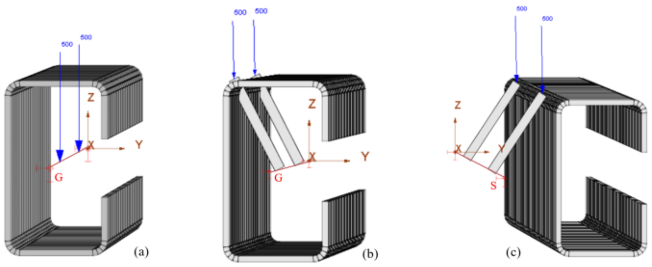

Figure 4 Representative finite element models for the three considered situation: (a) coincidence of both SL and LL (here at G), (b) SL passing through the gravity centre while LL is passing here through TLE (c) SL passing through the shear centre while LL here is passing through point TLE

For the last two situations, a rigid element has been used to link the point where the load is introduced and the support line. It has been observed that the rigidity of these elements strongly affects the results. Therefore, a sensitivity analysis has been performed in order to select its stiffness which has been finally taken 100 times higher than the rigidity of the member.

The numerical results, $M_{cr,n}$ obtained with FINELG for the first study case are summarized in Table 3 for all the loading positions (N° 1 to 6, as in Table 2). In order to further investigate the influence of the load eccentricity along y-y axis (see Figure 3 for the definition of the axis), six extreme and quite theoretical loading positions have been considered (N° 7a to 9b in Table 3) where the load was applied far away from the cross-section area, as shown in Figure 3, at:

7. ±100mm from the centre of gravity and acting on a plane perpendicular to y-y axis (GR and GL points respectively);
8. ±100mm from the centre of gravity but at the level of the top flange (TFR and TFL);
9. ±100mm from the centre of gravity but at the level of the lower flange (BFR and BFL).

Table 3 Numerical values of the elastic critical moment for the first study case, obtained with the FINELG software for the three considered situations

N°	Sit. a		Sit. b (axis at G)		Sit. c (axis at S)	
	$M_{cr,n}$ [kNm]	$\frac{M_{cr,n}}{M_{cr,an}}$	$M_{cr,n}$ [kNm]	$\frac{M_{cr,n}}{M_{cr,an}}$	$M_{cr,n}$ [kNm]	$\frac{M_{cr,n}}{M_{cr,an}}$
1	0.61	0.99	0.61	0.99	-	-
2	0.61	0.98	-	-	0.61	0.99
3	0.51	0.98	0.51	0.98	0.51	0.99
4	0.51	0.98	0.51	0.98	0.51	0.98
5	0.71	0.98	0.71	0.98	0.71	0.98
6	0.71	0.98	0.71	0.98	0.71	0.98
7a	0.60	0.98	0.61	0.99	0.61	0.99
7b	0.60	0.98	0.60	0.98	0.6	0.98
8a	0.51	0.99	0.51	0.99	0.51	0.99
8b	0.51	0.98	0.51	0.98	0.50	0.98
9a	0.71	0.98	0.71	0.98	0.71	0.98
9b	0.71	0.98	0.71	0.98	0.71	0.98

In Table 3, it can be easily seen that the elastic critical moment is not affected by the horizontal position of the applied load, even if the eccentricity associated to the relative position of the load along the y-y axis generates a torsional moment in the member. It may therefore be concluded that a first order torsional moment has no effect on the elastic lateral-torsional critical load. On the contrary, the vertical position of the load is influencing the elastic critical moment. In fact, placing the load above the shear centre will increase the rotation of the cross-section due to the eccentricity that arises as soon as the cross-section starts to twist and has therefore destabilizing effect whereas the same load acting on the bottom flange tends to stabilize the section as the rotation of the cross-section will be counteracted by the load. This can be easily explained when the profile is loaded perpendicularly to its major axis in the plane going through its shear centre. In all the other loading cases (load applied at the upper/bottom flange), the rotation of the beam (clockwise or opposite) brings or not this stabilizing effect (see Figure 5).

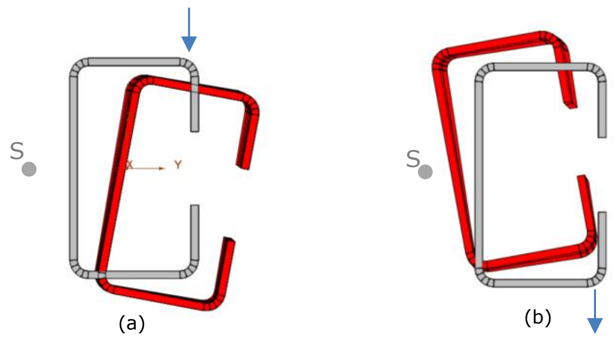

Figure 5 Buckling mode deformation when the load is applied (a) at the upper flange and has a destabilizing effect and (b) at the bottom flange where stabilizes the beam

By comparing both numerical and analytical results, it can be seen that Equation (1) predicts with high accuracy the elastic critical moment for all the considered situations; the mean value of the ratio $M_{cr,n}/M_{cr,an}$ as well as its standard deviation, which is negligible are reported in Table 4.

Table 4 Mean value and standard deviation of the ratio $\frac{M_{cr,n}}{M_{cr,an}}$ for the three different situations for the first study case

	Sit. a	Sit. b	Sit. c
Mean value [-]	0.98	0.98	0.98
Standard deviation [%]	0.36	0.34	0.34

Although no local or distortional buckling was expected to occur for the selected profile according to [1], it has been decided to perform some numerical simulations by means of Abaqus software, to ensure that these possible buckling modes are not effectively appearing. Therefore, the same beam has been modelled using solid finite elements and assuming that both SL and LL coincide (corresponding to the above-mentioned situation (a)). In addition, two types of solid elements have been selected (i.e., linear and quadratic) in order to investigate their influence on the member's response. The beam has been modelled with at least 3 volume elements over its thickness for both type of elements. To simulate the support conditions and to apply loads at points which do not belong to the member (i.e., at the gravity or the shear centre see Figure 6), a "pin" constraint has been implemented.

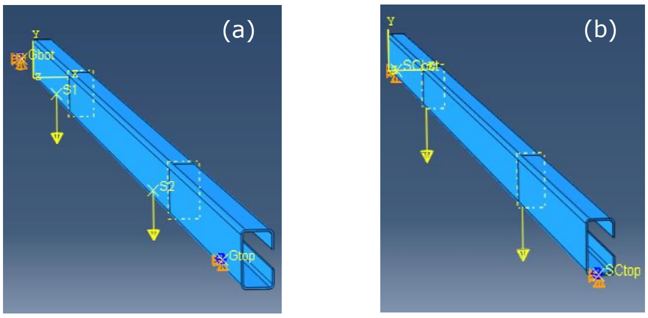

Figure 6 Finite element model with Abaqus software for the cases where the member is loaded at (a) the shear centre and (b) the bottom flange

It can be observed in Table 5 that both finite elements provide similar results, but the quadratic ones are closer to the analytical ones. The mean value of the ratio $M_{cr,FEM}/M_{cr,an}$, where $M_{cr,FEM}$ is the elastic critical moment obtained numerically with ABAQUS, is equal to 0.98 with a cov of 0.39% for quadratic elements in contrast with the linear ones where the mean value equals 0.96 and the standard deviation is 0.19%.

Table 5 Numerical evaluations of the elastic critical moment with ABAQUS software using two types of elements

N°	Position of loading	Linear FEM		Quadratic FEM	
		$M_{cr,FEM}$ [kNm]	$\frac{M_{cr,FEM}}{M_{cr,an}}$	$M_{cr,FEM}$ [kNm]	$\frac{M_{cr,FEM}}{M_{cr,an}}$
1	S	0.59	0.96	0.60	0.98
2	G	0.59	0.96	0.60	0.97
3	TLE	0.50	0.96	0.51	0.98
4	TRE	0.50	0.95	0.51	0.98
5	BLE	0.69	0.95	0.70	0.97
6	BRE	0.69	0.96	0.71	0.98

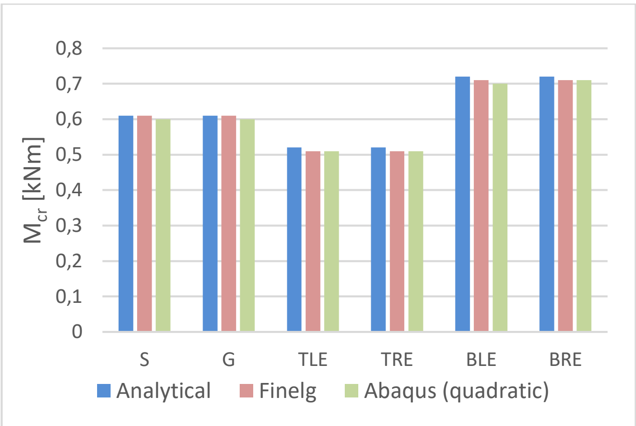

Figure 7 Comparison of the elastic critical moments obtained analytically and numerically for the first case study

Lastly, Figure 7 presents the different values of the elastic critical moment obtained with FINELG and ABAQUS for situation (a), for each of the six loading points. It can be observed that, for each case, the elastic critical moments obtained analytically and numerically are quite similar, with the numerical results to be always slightly lower than the analytical ones.

3.2 Case study 2

3.2.1 *Analytical calculations*

In the second case, a beam subjected to a constant bending moment at its extremities has been considered, with the same profile (see Table 1 for the geometrical properties and the support conditions). Obviously, as $C_2 \cdot z_g = 0$, a similar value of the analytically determined critical moment $M_{cr,an}$ is obtained for all the previously defined loading positions 1 to 6. As for the first study case, k_z and k_w were equal to 1.0; for a constant moment, the coefficient C_1 was taken equal to 1.0. As a result, the elastic critical moment $M_{cr,an}$ equals 0.59 kNm.

3.2.2 *Numerical simulations*

For this second study case, the same six loading points have been considered. The analyses have been performed with the ABAQUS software using quadratic solid finite elements. As it has been shown through the first study case, this type of finite elements gives more accurate results compared to the analytical ones; the results are reported in Table 6.

Table 6 Analytical and numerical evaluations (ABAQUS software) of M_{cr} for a constant applied moment

N°	Position of loading	Analytical formula	Situation a	
		$M_{cr,an}$ [kNM]	$M_{cr,FEM}$ [kNm]	$\frac{M_{cr,FEM}}{M_{cr,an}}$
1	S	0.59	0.57	0.97
2	G	0.59	0.57	0.97
3	TLE	0.59	0.57	0.97
4	TRE	0.59	0.57	0.97
5	BLE	0.59	0.57	0.97
6	BRE	0.59	0.57	0.97

Again, from both numerical and analytical results, it can be concluded that Equation (1) predicts with high accuracy the elastic critical moment also for the case where the beam is subjected to end bending moments and, as expected, is independent of the position of the applied load at the extremities of the beam (as the term $C_2 \cdot z_g = 0$).

4 Conclusions

This paper focuses on the lateral-torsional buckling (LTB) of beams with monosymmetric sections about their strong axis that are loaded perpendicularly to this axis of symmetry, and, in particular, on channel thin-walled cold-formed sections. Through this study which involves analytical and numerical studies, the following conclusions may be drawn:

- EN 1993-1-3 and prEN1993-1-3 give identical provisions regarding the LTB of cold-formed thin-walled sections;
- The formula given in CEN/TR 1993-1-103 for monosymmetric about their major axis sections predicts with high accuracy the elastic critical moment not only for the case where the load is introduced in the plane going through the shear centre of the section, but also for the practical cases where the load is imposed in the beam either through its web or the flanges; an amendment should accordingly be brought in CEN/TR 1993-1-103 so to extend the scope of application of Equation (1) where the text should be modified as follows "*beams with uniform cross-sections, symmetrical about the major axis loaded perpendicular to their major axis";*
- It has been shown that the vertical position of the load strongly influences the critical load while the horizontal one has no effect on the evaluation of the critical moment;
- The two considered software where different types of elements have been used provide results quite close to the analytical ones;
- The use of solid quadratic solid finite elements provides better results than those obtained by means of linear finite elements; obviously beam elements are also adequate as far as no local or distortional buckling occurs.

As part of this study, an experimental campaign aimed at studying the stability of beam in real structures is in progress, but the results are not available at the time of the publication of the present article. The final objective will be to propose and validate a complete design process for monosymmetric channel and sigma cold-formed beams subjected to bending.

Acknowledgement

The results of the study presented here have been carried out in the framework of research founded by the Walloon Region (SPW – Belgium). The industrial partners of this project are CRM group, GDTech and Stow international. The authors are grateful for this funding.

References

[1] EN 1993-1-3. Eurocode 3: Design of steel structures - Part 1-3: *General rules – Supplementary rules for cold-formed members and sheeting*, Brussels, Comité Européen de Normalisation (CEN), 2006.

[2] EN 1993-1-1: Design of steel structures - Part 1-1: *General rules and rules for buildings*, Brussels, Comité Européen de Normalisation (CEN), 2005

[3] CEN/TR 1993-1-103: Design of steel structures - Part 1-103: *Elastic critical buckling of members*, Brussels, Comité Européen de Normalisation (CEN), 2019

[4] Subotic, P.; Lucic, D. (2019) *Overview of the methods for calculating elastic critical LTB moment*, 7th international conference on Contemporary achievements in civil engineering, 23-24 April, Serbia.

[5] Timoshenko, S.P.;. Gere, J.M. (1961) *Theory of Elastic Stability*, McGraw-Hill, International Student Edition.

[6] Galéa, Y. (20a06) *Moment critique de déversement d'une poutre soumise à des moments d'extrémité et une charge uniforme: proposition d'une formulation analytique de C1 et C2,* Revue Construction Métallique 4, pp. 61–72.

[7] Seah, L.K.; Khong, P.W. (1990) *Lateral-torsional buckling of channel beams*, J. Constr. Steel Res. Vol. 17 (4), pp. 265–282.

[8] Shan-shan, C.; Boksun, K.; Long-yuan, L. (2013) *Lateral–torsional buckling of cold-formed channel sections subject to combined compression and bending*, Journal of Constructional Steel Research, vol.80, pp. 174–180.

[9] Horacek, M.; Melcher, J.; Pesek, O.; Brodniasky, J. (2016) *Focusing on problem of lateral torsional buckling of beams with web holes*, Procedia Engineering, Vol. 161, pp 549-555.

[10] Melcher, J.; Karmazinova, M. (2010) *Lateral buckling of steel sigma-cross-sections beams with web holes*, SDSS'Rio 2010 stability and ductility of steel structures conference.

[11] Beyer, A., Boissonnade, N.; Khelil, A.; Bureau, A. (2017) *Elastic instability of U-shaped members in bending considering pre-buckling displacements*, Journal of constructional steel research, Vol. 135 pp. 230-241.

[12] prEN 1993-1-3. Eurocode 3: Design of steel structures - Part 1-3: General rules - *Supplementary rules for cold-formed members and sheeting*, Brussels, Comité Européen de Normalisation (CEN), 2020

[13] pr EN 1993-1-1: Design of steel structures - Part 1-1: *General rules and rules for buildings*, Brussels, Comité Européen de Normalisation (CEN), 2019.

[14] FINELG: Non-linear finite element analysis program, User's manual, Version 9.0, Greisch Ingenieur, 2003.

[15] ABAQUS, User's manual, Version 6.14, Simulia, 2014

[16] Boissonade, N.; Greiner,R.; Jaspart, JP.; Lindner, J. (2006). *New design rules in EN1993-1-1 for member stability,* ECCS Technical Committee 8 – Structural stability, P119, ECCS, Brussels